





## 2 Experimental

Experiments were conducted using a 5.5 m<sup>3</sup> Teflon photochemical reaction chamber equipped with a mixing fan and UV lights (maximum output at 340 nm), described previously by Chen et al. (1998) and Lockwood et al. (2010). Three sets of experiments containing different seed aerosol conditions were completed as a function of chamber relative humidity: acidic seed, neutral seed, and the case without seed aerosol. The various seed aerosol types were created using an aerosol generator (3076, TSI, Inc.) and its output was passed through a Kr-85 aerosol neutralizer (TSI, Inc.) before injection into the chamber. A 15 mM (NH<sub>4</sub>)<sub>2</sub>SO<sub>4</sub> aerosol generator solution was used for the neutral seed aerosol experiments and a 30 mM MgSO<sub>4</sub>/50 mM H<sub>2</sub>SO<sub>4</sub> solution was used for the acidic seed aerosol experiments. The seed aerosol conditions were based on Surratt et al. (2008). Hydrogen peroxide, the OH radical precursor, and ultra-pure water were gently bubbled into the chamber under hydrocarbon-free air before the addition of the seed aerosol and  $\alpha$ -pinene. Chamber water concentrations were measured using a LICOR-7000. The  $\alpha$ -pinene (98 %, Sigma Aldrich, Inc.) was introduced into the chamber by injection through a glass tee under heat while nitric oxide was similarly injected under N<sub>2</sub> without heat.

Real time measurements were made using several instruments. The  $\alpha$ -pinene concentrations were measured using a gas chromatograph-flame ionization detector (GC-FID; HP-5980), NO/NO<sub>y</sub> concentrations were measured with a Thermo NO/NO<sub>y</sub> detector (Model 42, Thermo, Inc.), and a scanning mobility particle sizer (3062, TSI, Inc.) was used to determine size-resolved particle concentrations. Nitric oxide concentrations were kept above 100 ppb to keep ozone concentrations low and ensure the hydroxyl radical was the sole initial oxidizing agent. Selected experiments were conducted using isooctane as a relative rate compound to determine that OH radical concentrations in the chamber ranged from  $1 \times 10^6 \text{ cm}^{-3}$  to  $1 \times 10^7 \text{ cm}^{-3}$ .

After injection, the contents of the chamber were allowed to mix for 10 min before the fan was turned off for the duration of the experiment. The experiment was initiated

3305

(time = 0) when the UV lamps were turned on and the experiment was terminated when approximately half of the initial  $\alpha$ -pinene was consumed, in an effort to focus on first generation products. Typical experiment lengths were one hour. All sampling lines were heated PFA Teflon (120 °C) except for the copper aerosol sampling line. The chamber was flushed continuously with at least five chamber volumes of hydrocarbon-free air prior to each experiment.

Denuder-based filter samples were acquired at the completion of each experiment for off-line analysis. Gas phase compounds were sampled at 10 L min<sup>-1</sup> and adsorbed onto the surface of the XAD-4 coated annular denuder (20 cm, URG, Inc.) while particle phase compounds were collected on a filter pack containing a Teflon filter (47 mm, VWR, Inc.) and a carbon-infused back-up filter (Grade 72, VWR, Inc.), which is used to capture gas phase negative artifacts arising from the front filter. The gas phase collection efficiency was determined by measuring the concentration of an isopropyl nitrate standard (99 %, Sigma Aldrich) both upstream and downstream of the denuder. The collection efficiency was  $\geq 98 \%$ . The denuder was extracted in a 50 : 30 : 20 acetonitrile : hexane : methylene chloride solution and extracts were dried to  $\sim 50 \%$  of their original volume before transfer to tetrachloroethylene (C<sub>2</sub>Cl<sub>4</sub>) to prevent losses during drying. Filters were placed in tetrachloroethylene and sonicated for 45 min. Blank samples were acquired from the chamber prior to the experiment using only the filter pack.

Organic nitrate quantification was accomplished through use of a Bruker Tensor FT-IR spectrometer (Bruker, Inc.). FT-IR has been successfully employed in several previous laboratory and field studies for organic nitrate quantification (Laurent and Allen, 2004; Dekermenjian et al., 1999; Noda et al., 2000; Hallquist et al., 1999; Nielsen et al., 1998). Filter and denuder extracts were analyzed in a 1 cm liquid cell and organic nitrate concentrations were determined using the asymmetric -NO<sub>2</sub> stretch at  $\sim 1640 \text{ cm}^{-1}$ , unique to organic nitrates (Nielsen et al., 1995). Typical spectra for both a filter extract and blank extract in C<sub>2</sub>Cl<sub>4</sub> are shown in Fig. 1. While traditionally there are three distinct bands used to quantify organic nitrate in the infrared spectrum (1645,

3306



branching ratio. The  $26 \pm 7\%$  total organic nitrate yield reported here is higher than the  $\sim 1\%$  reported by Aschmann et al. (2002) but does not statistically differ from the  $18 \pm 9\%$  determined by Noziere et al. (1999), who also used FT-IR to determine organic nitrate concentrations. Additionally, as shown in Fig. 5, our reported yield value is consistent with the VOC size-dependent alkyl nitrate branching ratio described previously (Arey et al., 2001). Although this trend in organic nitrate yield has been shown to plateau for VOCs with high carbon numbers, the  $C_{10}$  system studied here is below the expected carbon number limit ( $\sim C_{15}$ ) for such a plateau to occur (Matsunaga and Ziemann, 2010).

The organic nitrate contribution to total particle mass was also determined for experiments in the 0–20% RH range. As stated previously, this calculation, which is the ratio of total organic nitrate mass in the particle phase to the total SOA mass produced, could only be assessed for seeded aerosol experiments as the final aerosol mass concentrations for unseeded experiments could not be determined. The calculated mass fraction of organic nitrates in the particle phase, assuming an organic nitrate molecular weight of  $215 \text{ g mol}^{-1}$ , is  $18 \pm 4\%$  for the seeded aerosol experiments, the same value (18%) reported by Rollins et al. (2010) from an  $\alpha$ -pinene/ $\text{NO}_x$  irradiation flow-tube study in the absence of seed aerosol.

### 3.1.2 Humidity dependence of organic nitrate yields

Organic nitrate yield experiments were conducted with chamber relative humidity ranging from 0 to  $\sim 90\%$  RH for each set of seed aerosol conditions. The total organic nitrate yields were highly dependent on chamber relative humidity, as seen in Figs. 3 and 4. The total (gas + particle phases) organic nitrate yield decreased rapidly as RH was increased from 0 to  $\sim 20\%$  in both the unseeded and seeded aerosol conditions, followed by a less pronounced drop from 20–90% RH to yields as low as 5%. In Fig. 6, we show the gas phase and aerosol phase yields separately for the acidic seed case. Despite our lack of knowledge of the relationship between aerosol liquid water content of the SOA created and chamber relative humidity, the strong inverse correlation be-

3309

tween organic nitrate concentration and the presence of water vapor within the chamber indicates that the SOA particles created may have a high potential for water uptake, leading to organic nitrate hydrolysis in the particle phase. Hydrolysis of organic nitrates has been previously reported for aqueous phase laboratory studies (Darer et al., 2011; Hu et al., 2011) and is believed to be responsible for decreased organic nitrate aerosol concentrations in a recent chamber study (Liu et al., 2012). Our findings add further evidence for the importance of the hydrolysis reaction in particle phase chemistry and helps provide an explanation for the decrease in organic nitrogen-containing species observed at high ambient RH in a recent field study (Day et al., 2010). The decrease in organic nitrate yields with humidity was observed with all three types of seed aerosol experiment sets.

A reaction mechanism for the proposed condensed phase hydrolysis of an  $\alpha$ -pinene-derived nitrate at neutral pH is shown in Scheme 2. The hydrolysis mechanism to form the corresponding alcohol likely proceeds via unimolecular nucleophilic substitution ( $S_N1$ ) rather than bimolecular nucleophilic substitution ( $S_N2$ ) as suggested previously (Darer et al., 2011). Instead of occurring in a single step initiated by nucleophilic attack, the  $S_N1$  mechanism occurs in two separate steps where first the leaving group, in this case the nitrate anion, detaches from the molecule to form a carbocation, which is followed by the attachment of the nucleophile, in this case water, at the available site. As water is a weak nucleophile, it is more likely that it will attach to an available carbocation rather than attack a carbon center carrying a weakly induced dipole. Previous laboratory studies indicate that tertiary organic nitrates are much more susceptible to hydrolysis than similar primary species (Darer et al., 2011). This phenomenon is consistent with the  $S_N1$  mechanism as the steric hindrance of tertiary organic compounds makes it difficult for an  $S_N2$  transition state to exist. Also, the carbocation intermediates formed from tertiary organics are much more stable than their primary counterparts, allowing for much faster  $S_N1$  reaction rates. As the major organic nitrate products produced from this oxidation pathway are expected to be both tertiary and secondary (Scheme 3), partitioning to and hydrolysis in the particle phase is a feasible

explanation for decreased organic nitrate yields as a function of chamber humidity. Unfortunately, standards are unavailable for the expected organic nitrate products and the applicable aqueous phase lifetimes are currently unknown. The reported lifetimes for tertiary  $\beta$ -hydroxy-organic nitrates in the aqueous phase are less than one hour (Darer et al., 2011), which would fall within the experimental timescale. However, a recent chamber study investigating the hydrolysis of trimethylbenzene-derived organic nitrate compounds, which were predicted to be primarily tertiary organic nitrates, reported a particle phase lifetime of  $\sim 6$  h (Liu et al., 2012).

Further evidence to support organic nitrate hydrolysis via the  $S_N1$  mechanism is shown by the difference in organic nitrate yields between the neutral and the acidic seed aerosol experiments as chamber RH was increased. The particle phase organic nitrate yields in the acidic seed case decreases much more rapidly than the neutral seed case (see Fig. 3 for the total yields), falling to nearly 0% at high RH (Fig. 6), while the particle organic nitrate yields only dropped to  $\sim 4$ % in the neutral seed experiments at similar relative humidity. The gas phase yields were not dependent on seed aerosol composition. The dependence of the organic nitrate yield on both chamber water content and seed aerosol acidity supports the proposed mechanism as organic nitrate hydrolysis rates are known to increase with solution acidity (Hu et al., 2011), providing evidence that reactions that eliminate the  $RONO_2$  functionality, such as hydrolysis, are acid-catalyzed. Additionally, the aqueous acidic conditions in this study provide a polar protic solvent system which favors  $S_N1$  and E1 mechanisms by allowing for increased stabilization of the transition state and better solvation of the leaving group, leading to an increase in both carbocation formation and product creation. Since the formation of the carbocation is the rate determining step of this reaction, the hydrolysis mechanism should be a first order process, consistent with previously reported data (Hu et al., 2001).

In the case of the unseeded aerosol experiments, the total organic nitrate yield showed a similar trend as the seeded aerosol experiments when RH was increased (Fig. 4). If the degree of organic nitrate hydrolysis within the timescale of these exper-

3311

iments is related to particle acidity, the behavior of the unseeded variable yield plot must be influenced by the uptake of  $HNO_3$  to the particle phase, produced either in the gas phase (Reaction R7) or at the surface (Atkinson et al., 1976; Murdachaew et al., 2013).



### 3.1.3 Gas-particle partitioning of monoterpene-derived organic nitrates

Using denuder-based filter sampling allowed for separate analysis of both the gas and particle phase products. Results indicate that for the high aerosol loadings in these experiments, much of the organic nitrate mass is in the particle phase. The average  $F_i/A_i$  ratio of organic nitrates in the system, where  $F_i$  and  $A_i$  are the particle and gas phase concentrations, respectively, was greater than 1.0 for all experiments when the chamber was dry (RH < 20%). When chamber humidity was increased to > 20% RH, only the acidic seed scenario decreased in average  $F_i/A_i$  ratio below 1.0, which is consistent with more facile consumption of the organic nitrate in the particle phase under acidic conditions. This phenomenon is likely the result of an acid-induced increase in the rate of hydrolysis in the particle phase to a rate that out-competes uptake of gas phase organic nitrates into the aerosol phase. To estimate an upper limit for the rate of  $RONO_2$  loss in our system via particle phase hydrolysis, the uptake rate ( $R_{in}$ ) of organic nitrates was calculated using Eq. (1) described by Jacob (2000), where  $r$  is the radius of the particle,  $D_g$  is the gas-phase molecular diffusion coefficient,  $v$  is the mean molecular speed,  $\alpha$  is the  $RONO_2$  mass accommodation coefficient,  $A$  is the aerosol surface area per unit volume of air, and  $N'$  is the gas phase  $RONO_2$  concentration. Assuming a mass accommodation factor ( $\alpha$ ) similar to that for 2-nitrophenol, 0.012 (Muller and Heal, 2002), a  $D_g$  of  $0.2 \text{ cm}^2 \text{ s}^{-1}$  (Jacob, 2000), and a calculated  $v$  of  $1.72 \times 10^4 \text{ cm s}^{-1}$ , the estimated timescale for uptake into the aerosol phase,  $\tau_{\text{uptake}} (R_{in}/N')$ , was calculated to be 194 s. That value, the lower limit timescale for the loss of  $RONO_2$  in our system after partitioning to the particle phase, is much shorter than

3312

the total experimental and sampling timescale of  $\sim 2.5$  h.

$$R_{\text{in}} = \left( \frac{r}{D_g} + \frac{4}{v\alpha} \right)^{-1} AN' \quad (1)$$

To further examine the partitioning of the organic nitrates as a function of aerosol type and humidity, partition coefficients were calculated based on Pankow (1994), which  
5 assumes a reversible gas-particle partitioning process involving solubilization of the gas phase component throughout the particle (Eq. 2). Plotting the  $F_i/A_i$  ratio against the total aerosol mass ( $M$ ) should yield a slope equal to the partition coefficient ( $K_p$ ) for a system in equilibrium. The resulting plot is highly scattered and does not show such a relationship, implying that partitioning is highly variable in the system (or that  
10  $F_i/A_i$  is dependent on variables other than  $M$ ) and cannot be explained by a simple gas-particle equilibrium partitioning model.

$$K_p = \frac{F_i/M}{A_i} \quad (2)$$

Support of an apparent non-equilibrium partitioning system can be seen by examining the decrease in both the gas and particle organic nitrate yields as a function of  
15 RH in the acidic seed aerosol case. Particle phase organic nitrate yields decreased to  $\sim 0\%$  at high humidity ( $> 60\%$  RH) while the apparent gas phase yields decreased to  $\sim 6\%$  (Fig. 6). Calculated partition coefficients are shown in Fig. 7. We note that at high humidity, the decrease in apparent  $K_p$  is greater than implied by the data shown in Fig. 7, because for elevated chamber RH (see Fig. 6), the aerosol phase  $\text{RONO}_2$  concentration was below the detection limit, and these cases are not plotted. The decrease  
20 in apparent particle phase organic nitrate yields can be explained by hydrolysis in the aerosol phase. Then, to maintain equilibrium, uptake of gas phase organic nitrates to the particle phase will occur, where loss continues. The consumption of organic nitrates

3313

in the particle phase via hydrolysis perturbs the equilibrium of the system, causing further partitioning of gas phase organic nitrates into the particle phase, followed by subsequent hydrolysis, lowering the apparent yields for both phases, as shown in Fig. 7, which shows the calculated apparent  $K_p$  values varied over three orders of magnitude.  
5 The calculated partition coefficients were larger at low RH than at high RH for both the neutral and acidic seed cases. We note that the condensed phase chemical reaction of organic nitrates to form less volatile species within aerosols also is likely to contribute to the observed apparent non-equilibrium partitioning.

Another factor that may contribute to the observed partitioning is the physical property of the aerosol particle. Recent work has shown that particles can range from “hard”  
10 and viscous at low humidity to much “softer” at higher RH where water uptake occurs much more readily (Shiraiwa et al., 2012; Virtanen et al., 2010; You et al., 2012). A previous organic nitrate partitioning study attributed an observed apparent non-equilibrium system to such effects while at very low RH (Perraud et al., 2012). Thus, at low RH, the particles may have a high viscosity, limiting uptake to the bulk particle and contrasting the Pankow model. At high RH the viscosity may be lower due to higher liquid water content and solvation of the particle phase oxidation products, which may lead to an increase in polar solute dissolution within the particle and hydrolysis chemistry. Thus, there can be multiple variables that affect partitioning as a function of RH.

Under typical tropospheric conditions, hydrolysis will likely be important as relative humidity is most often above the range where this study began to observe  $\text{RONO}_2$   
15 hydrolysis (0–10% RH), meaning that water interaction with SOA particles may occur even at very low RH and that multiple physical and chemical processes affect how low volatility organic nitrates, such as those derived from monoterpene oxidation, partition  
25 between the gas and aerosol phases.

### 3.1.4 Hydrolysis product identification

Despite the evidence for particle phase organic nitrate hydrolysis, the formation pathway of  $\alpha$ -pinene-derived nitrates and the mechanisms that govern their fate still remain

3314

uncertain due to the lack of standards for specific reaction products in both the gas and aerosol phases. A likely product of the hydrolysis of the  $\alpha,\beta$ -hydroxy-organic nitrates derived from  $\alpha$ -pinene, pinanediol (Scheme 2), was not observed in any denuder or filter extracts using GC-MS and a commercially available standard (Sigma Aldrich, Inc.).

5 One explanation for the lack of observed pinanediol is that rearrangement can occur in a reaction intermediate. As outlined by Peeters et al. (2001) and shown in Scheme 3, radical rearrangement can occur after the addition of the hydroxyl radical across the double bond of  $\alpha$ -pinene, leading to different organic nitrate isomers than those expected to be precursors for  $\alpha,\beta$ -pinanediol. A similar rearrangement can occur during hydrolysis after the nitrate leaving group detaches from the organic nitrate to form the carbocation intermediate through the  $S_N1$  mechanism. Both rearrangement pathways would lead to other  $C_5H_{12}O_2$  isomer (or other) products than pinanediol. Additionally, it is possible for other chemical mechanisms to govern the fate of organic nitrate species in the condensed phase, such as elimination to form an olefinic product, or cleavage of the O–N bond to create a carbonyl compound (Baker and Easty, 1950). However, since these alternative scenarios involve either  $\alpha$ - or  $\beta$ -hydrogen abstraction, they may not be strong candidates for the consumption of tertiary organic nitrates under acidic conditions. Nonetheless, when considering the fate of tertiary organic nitrates, the E1 elimination mechanism via  $\beta$ -hydrogen abstraction will be in direct competition with the  $S_N1$  mechanism, the importance of which should be explored (Scheme 5). Further investigation into the organic nitrate hydrolysis mechanism at low pH is needed.

15 Another explanation relates to the degree of reactivity that exists in the particle phase. For instance, pinanediol could undergo further reactions, such as oligomerization, sulfate esterification, substitution or elimination mechanisms to produce new products. Example reactions are shown in Scheme 4. Additionally, recent literature has shown that pinanediol can undergo extensive oxidation in nucleation events to form both highly oxidized dimers as well as  $C_{10}$ -compounds with O : C ratios as high as 1 : 1 (Schobesberger et al., 2013). Also of note, recent literature by Rollins et al. (2012) sug-

3315

gests that multigenerational organic nitrates are responsible for SOA formation, meaning that at least some of the aerosol phase organic nitrates measured in this study may be more complex oxidation products than those originally created from the reaction of NO with the first generation peroxy radicals (Reaction R3a).

5 The lack of detected pinanediol in this study highlights the need for further study of the condensed phase chemistry of monoterpene oxidation products. The application of new analytical techniques and/or authentic standards is needed to elucidate the chemical mechanisms of organic nitrate formation and fate in the condensed phase.

### 3.2 Atmospheric implications

10 The high degree of organic nitrate partitioning and hydrolysis in the particle phase, even under low RH conditions, may have an important impact on  $NO_x$ ,  $O_3$ , and regional air quality. Organic nitrates may be a sink for gas phase  $NO_x$ ; however, further reactions, such as oxidation or photolysis in either the gas or particle phase, may release  $NO_x$  back into the gas phase, leading to an effectively longer  $NO_x$  lifetime. The transformation of organic nitrates to the analogous alcohol within the aerosol will convert the nitrooxy group in the organic nitrate to the nitrate ion, which will remain relatively longer (depending on pH) in the particle phase due to its lower reactivity. For instance, organic nitrate photolysis rates are at least a couple orders of magnitude faster than those for the nitrate ion (Suarez-Bertoa et al., 2012; Zafiriou and True, 1979; Galbavy et al., 2007). This production of the nitrate ion would eliminate the possibility for further oxidation of organic nitrates and the release of  $NO_x$ . Thus, deposition of the nitrate ion would be the main pathway of  $\alpha$ -pinene-derived nitrate removal from the atmosphere, and the relatively large organic nitrate yield from a monoterpene reported here (26 ± 7 %), along with fast hydrolysis in the aerosol phase, likely makes organic nitrate production in coniferous forests an important sink for  $NO_x$ , limiting ozone production. The organic nitrate yield values, partition coefficients, and hydrolysis rate constants would then be important components needed to assess  $NO_x$  sequestration and nitrogen deposition.

3316





- Eddingsaas, N. C., Loza, C. L., Yee, L. D., Chan, M., Schilling, K. A., Chhabra, P. S., Seinfeld, J. H., and Wennberg, P. O.:  $\alpha$ -pinene photooxidation under controlled chemical conditions – Part 2: SOA yield and composition in low- and high-NO<sub>x</sub> environments, *Atmos. Chem. Phys.*, 12, 7413–7427, doi:10.5194/acp-12-7413-2012, 2012.
- 5 Galbavy, E. S., Anastasio, C., Lefer, B., and Hall, S.: Light penetration in the snowpack at Summit, Greenland: Part 2 nitrate photolysis, *Atmos. Environ.*, 41, 5091–5100, doi:10.1016/j.atmosenv.2006.01.066, 2007.
- Goldstein, A. H. and Galbally, I. E.: Known and unexplored organic constituents in the Earth's atmosphere, *Environ. Sci. Technol.*, 41, 1514–1521, doi:10.1021/es072476p, 2007.
- 10 Guenther, A. B., Jiang, X., Heald, C. L., Sakulyanontvittaya, T., Duhl, T., Emmons, L. K., and Wang, X.: The Model of Emissions of Gases and Aerosols from Nature version 2.1 (MEGAN2.1): an extended and updated framework for modeling biogenic emissions, *Geosci. Model Dev.*, 5, 1471–1492, doi:10.5194/gmd-5-1471-2012, 2012.
- Hallquist, M., Wangberg, I., Ljungstrom, E., Barnes, I., and Becker, K. H.: Aerosol and product yields from NO<sub>3</sub> radical-initiated oxidation of selected monoterpenes, *Environ. Sci. Technol.*, 15 33, 553–559, doi:10.1021/es980292s, 1999.
- Henry, K. M., Lohaus, T., and Donahue, N. M.: Organic aerosol yields from alpha-pinene oxidation: bridging the gap between first-generation yields and aging chemistry, *Environ. Sci. Technol.*, 46, 12347–12354, doi:10.1021/es302060y, 2012.
- 20 Hoffmann, T., Odum, J. R., Bowman, F., Collins, D., Klockow, D., Flagan, R. C., and Seinfeld, J. H.: Formation of organic aerosols from the oxidation of biogenic hydrocarbons, *J. Atmos. Chem.*, 26, 189–222, doi:10.1023/a:1005734301837, 1997.
- Hu, K. S., Darer, A. I., and Elrod, M. J.: Thermodynamics and kinetics of the hydrolysis of atmospherically relevant organonitrates and organosulfates, *Atmos. Chem. Phys.*, 11, 8307–8320, doi:10.5194/acp-11-8307-2011, 2011.
- 25 Iinuma, Y., Kahnt, A., Mutzel, A., Boge, O., and Herrmann, H.: Ozone-driven secondary organic aerosol production chain, *Environ. Sci. Technol.*, 47, 3639–3647, doi:10.1021/es305156z, 2013.
- Jacob, D. J.: Heterogeneous chemistry and tropospheric ozone, *Atmos. Environ.*, 34, 2131–2159, doi:10.1016/s1352-2310(99)00462-8, 2000.
- 30 Jaoui, M. and Kamens, R. M.: Mass balance of gaseous and particulate products analysis from alpha-pinene/NO<sub>x</sub>/air in the presence of natural sunlight, *J. Geophys. Res.-Atmos.*, 106, 12541–12558, doi:10.1029/2001jd900005, 2001.

3319

- Laurent, J. P. and Allen, D. T.: Size distributions of organic functional groups in ambient aerosol collected in Houston, Texas, *Aerosol Sci. Tech.*, 38, 82–91, doi:10.1080/02786820390229561, 2004.
- 5 Lee, A., Goldstein, A. H., Kroll, J. H., Ng, N. L., Varutbangkul, V., Flagan, R. C., and Seinfeld, J. H.: Gas-phase products and secondary aerosol yields from the photooxidation of 16 different terpenes, *J. Geophys. Res.-Atmos.*, 111, D17305, doi:10.1029/2006jd007050, 2006.
- Liu, S., Shilling, J. E., Song, C., Hiranuma, N., Zaveri, R. A., and Russell, L. M.: Hydrolysis of organonitrate functional groups in aerosol particles, *Aerosol Sci. Tech.*, 46, 1359–1369, 10 doi:10.1080/02786826.2012.716175, 2012.
- Lockwood, A. L., Filley, T. R., Rhodes, D., and Shepson, P. B.: Foliar uptake of atmospheric organic nitrates, *Geophys. Res. Lett.*, 35, L15809, doi:10.1029/2008gl034714, 2008.
- Matsunaga, A. and Ziemann, P. J.: Yields of beta-hydroxynitrates, dihydroxynitrates, and trihydroxynitrates formed from OH radical-initiated reactions of 2-methyl-1-alkenes, *P. Natl. Acad. Sci. USA*, 107, 6664–6669, doi:10.1073/pnas.0910585107, 2010.
- 15 Muller, B. and Heal, M. R.: Mass accommodation coefficients of phenol, 2-nitrophenol, and 3-methylphenol over the temperature range 278–298 K, *J. Phys. Chem. A*, 106, 5120–5127, doi:10.1021/jp013559+, 2002.
- Murdachaw, G., Varner, M. E., Phillips, L. F., Finlayson-Pitts, B. J., and Gerber, R. B.: Nitrogen dioxide at the air–water interface: trapping, absorption, and solvation in the bulk and at the surface, *Phys. Chem. Chem. Phys.*, 15, 204–212, doi:10.1039/c2cp42810e, 2013.
- Ng, N. L., Kroll, J. H., Keywood, M. D., Bahreini, R., Varutbangkul, V., Flagan, R. C., Seinfeld, J. H., Lee, A., and Goldstein, A. H.: Contribution of first- versus second-generation products to secondary organic aerosols formed in the oxidation of biogenic hydrocarbons, 25 *Environ. Sci. Technol.*, 40, 2283–2297, doi:10.1021/es052269u, 2006.
- Nguyen, T. B., Laskin, J., Laskin, A., and Nizkorodov, S. A.: Nitrogen-containing organic compounds and oligomers in secondary organic aerosol formed by photooxidation of isoprene, *Environ. Sci. Technol.*, 45, 6908–6918, doi:10.1021/es201611n, 2011.
- Nielsen, T., Egelov, A. H., Granby, K., and Skov, H.: Observations on particulate organic nitrates and unidentified components of NO<sub>y</sub>, *Atmos. Environ.*, 29, 1757–1769, doi:10.1016/1352-2310(95)00098-j, 1995.
- 30

3320

- Nielsen, T., Platz, J., Granby, K., Hansen, A. B., Skov, H., and Egelov, A. H.: Particulate organic nitrates: sampling and night/day variation, *Atmos. Environ.*, 32, 2601–2608, doi:10.1016/s1352-2310(97)00483-4, 1998.
- Noda, J., Hallquist, M., Langer, S., and Ljungstrom, E.: Products from the gas-phase reaction of some unsaturated alcohols with nitrate radicals, *Phys. Chem. Chem. Phys.*, 2, 2555–2564, doi:10.1039/b000251h, 2000.
- Nozriere, B., Barnes, I., and Becker, K. H.: Product study and mechanisms of the reactions of alpha-pinene and of pinonaldehyde with OH radicals, *J. Geophys. Res.-Atmos.*, 104, 23645–23656, doi:10.1029/1999jd900778, 1999.
- Pankow, J. F.: An absorption-model of gas-particle partitioning of organic-compounds in the atmosphere, *Atmos. Environ.*, 28, 185–188, doi:10.1016/1352-2310(94)90093-0, 1994.
- Paulot, F., Crouse, J. D., Kjaergaard, H. G., Kroll, J. H., Seinfeld, J. H., and Wennberg, P. O.: Isoprene photooxidation: new insights into the production of acids and organic nitrates, *Atmos. Chem. Phys.*, 9, 1479–1501, doi:10.5194/acp-9-1479-2009, 2009.
- Paulot, F., Henze, D. K., and Wennberg, P. O.: Impact of the isoprene photochemical cascade on tropical ozone, *Atmos. Chem. Phys.*, 12, 1307–1325, doi:10.5194/acp-12-1307-2012, 2012.
- Peeters, J., Vereecken, L., and Fantechi, G.: The detailed mechanism of the OH-initiated atmospheric oxidation of alpha-pinene: a theoretical study, *Phys. Chem. Chem. Phys.*, 3, 5489–5504, doi:10.1039/b106555f, 2001.
- Perraud, V., Bruns, E. A., Ezell, M. J., Johnson, S. N., Yu, Y., Alexander, M. L., Zelenyuk, A., Imre, D., Chang, W. L., Dabdub, D., Pankow, J. F., and Finlayson-Pitts, B. J.: Nonequilibrium atmospheric secondary organic aerosol formation and growth, *P. Natl. Acad. Sci. USA*, 109, 2836–2841, doi:10.1073/pnas.1119909109, 2012.
- Rollins, A. W., Smith, J. D., Wilson, K. R., and Cohen, R. C.: Real time in situ detection of organic nitrates in atmospheric aerosols, *Environ. Sci. Technol.*, 44, 5540–5545, doi:10.1021/es100926x, 2010.
- Rollins, A. W., Pusede, S., Wooldridge, P., Min, K. E., Gentner, D. R., Goldstein, A. H., Liu, S., Day, D. A., Russell, L. M., Rubitschun, C. L., Surratt, J. D., and Cohen, R. C.: Gas/particle partitioning of total alkyl nitrates observed with TD-LIF in Bakersfield, *J. Geophys. Res.-Atmos.*, 118, 6651–6662, doi:10.1002/jgrd.50522, 2013.
- Schobesberger, S., Junninen, H., Bianchi, F., Lonn, G., Ehn, M., Lehtipalo, K., Dommen, J., Ehrhart, S., Ortega, I. K., Franchin, A., Nieminen, T., Riccobono, F., Hutterli, M., Duplissy, J., Almeida, J., Amorim, A., Breitenlechner, M., Downard, A. J., Dunne, E. M., Fla-

3321

- gan, R. C., Kajos, M., Keskinen, H., Kirkby, J., Kupc, A., Kurten, A., Kurten, T., Laaksonen, A., Mathot, S., Onnela, A., Praplan, A. P., Rondo, L., Santos, F. D., Schallhart, S., Schnitzhofer, R., Sipila, M., Tome, A., Tsagkogeorgas, G., Vehkamäki, H., Wimmer, D., Baltensperger, U., Carslaw, K. S., Curtius, J., Hansel, A., Petaja, T., Kulmala, M., Donahue, N. M., and Worsnop, D. R.: Molecular understanding of atmospheric particle formation from sulfuric acid and large oxidized organic molecules, *P. Natl. Acad. Sci. USA*, 110, 17223–17228, doi:10.1073/pnas.1306973110, 2013.
- Shiraiwa, M., Ammann, M., Koop, T., and Poschl, U.: Gas uptake and chemical aging of semisolid organic aerosol particles, *P. Natl. Acad. Sci. USA*, 108, 11003–11008, doi:10.1073/pnas.1103045108, 2011.
- Shiraiwa, M., Pfrang, C., Koop, T., and Pöschl, U.: Kinetic multi-layer model of gas-particle interactions in aerosols and clouds (KM-GAP): linking condensation, evaporation and chemical reactions of organics, oxidants and water, *Atmos. Chem. Phys.*, 12, 2777–2794, doi:10.5194/acp-12-2777-2012, 2012.
- Smith, M. L., Bertram, A. K., and Martin, S. T.: Deliquescence, efflorescence, and phase miscibility of mixed particles of ammonium sulfate and isoprene-derived secondary organic material, *Atmos. Chem. Phys.*, 12, 9613–9628, doi:10.5194/acp-12-9613-2012, 2012.
- Suarez-Bertoa, R., Picquet-Varrault, B., Tamas, W., Pangui, E., and Doussin, J. F.: Atmospheric fate of a series of carbonyl nitrates: photolysis frequencies and OH-oxidation rate constants, *Environ. Sci. Technol.*, 46, 12502–12509, doi:10.1021/es302613x, 2012.
- Surratt, J. D., Gómez-González, Y., Chan, A. W. H., Vermeylen, R., Shahgholi, M., Kleindienst, T. E., Edney, E. O., Offenberg, J. H., Lewandowski, M., Jaoui, M., Maenhaut, W., Claeys, M., Flagan, R. C., and Seinfeld, J. H.: Organosulfate formation in biogenic secondary organic aerosol, *J. Phys. Chem. A*, 112, 8345–8378, doi:10.1021/jp802310p, 2008.
- Tuazon, E. C., Atkinson, R., Macleod, H., Biermann, H. W., Winer, A. M., Carter, W. P. L., and Pitts, J. N.: Yields of glyoxal and methylglyoxal from the NO<sub>x</sub>-air photooxidations of toluene and *m*-xylene and *p*-xylene, *Environ. Sci. Technol.*, 18, 981–984, doi:10.1021/es00130a017, 1984.
- Veselovskii, I. A., Cha, H. K., Kim, D. H., Choi, S. C., and Lee, J. M.: Raman lidar for the study of liquid water and water vapor in the troposphere, *Appl. Phys. B-Lasers O.*, 71, 113–117, 2000.
- Virtanen, A., Joutsensaari, J., Koop, T., Kannosto, J., Yli-Pirila, P., Leskinen, J., Makela, J. M., Holopainen, J. K., Poschl, U., Kulmala, M., Worsnop, D. R., and Laaksonen, A.: An amor-

3322

phous solid state of biogenic secondary organic aerosol particles, *Nature*, 467, 824–827, doi:10.1038/nature09455, 2010.

Worton, D. R., Mills, G. P., Oram, D. E., and Sturges, W. T.: Gas chromatography negative ion chemical ionization mass spectrometry: Application to the detection of alkyl nitrates and halocarbons in the atmosphere, *J. Chromatogr. A*, 1201, 112–119, doi:10.1016/j.chroma.2008.06.019, 2008.

You, Y., Renbaum-Wolff, L., Carreras-Sospedra, M., Hanna, S. J., Hiranuma, N., Kamal, S., Smith, M. L., Zhang, X. L., Weber, R. J., Shilling, J. E., Dabdub, D., Martin, S. T., and Bertram, A. K.: Images reveal that atmospheric particles can undergo liquid–liquid phase separations, *P. Natl. Acad. Sci. USA*, 109, 13188–13193, doi:10.1073/pnas.1206414109, 2012.

Zafiriou, O. C. and True, M. B.: Nitrate photolysis in seawater by sunlight, *Mar. Chem.*, 8, 33–42, doi:10.1016/0304-4203(79)90030-6, 1979.

3323

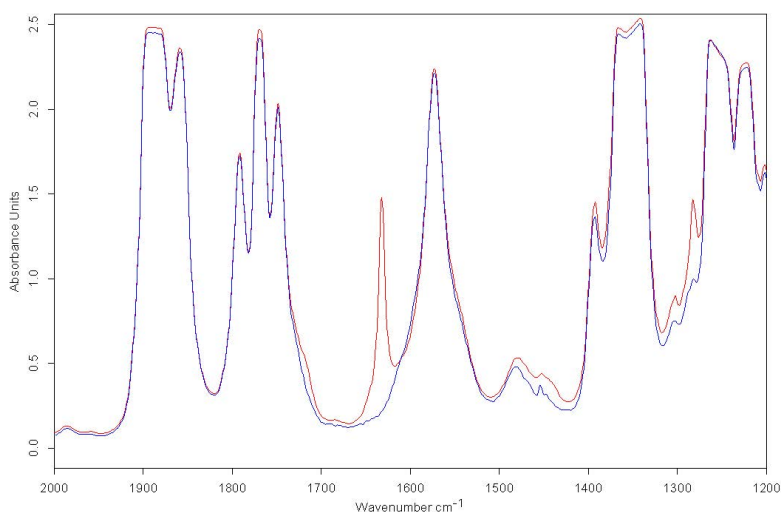


**Fig. 1.** The FT-IR spectra of a filter sample extracted in C<sub>2</sub>Cl<sub>4</sub> (red) and a filter blank (blue). The peak at ~ 1640 cm<sup>-1</sup> corresponds to the asymmetric -NO<sub>2</sub> stretch of organic nitrates.

3324

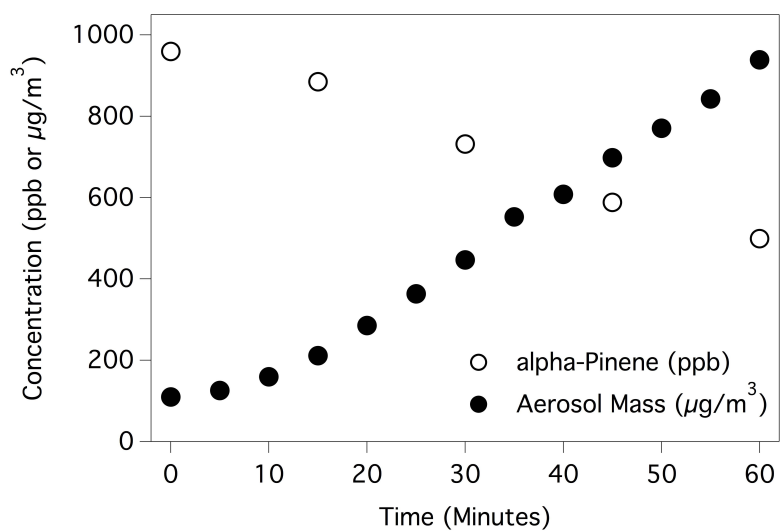


**Fig. 2.** The  $\alpha$ -pinene and aerosol mass concentrations as a function of time for a representative experiment. The open circles (○) represent  $\alpha$ -pinene (ppb) while the closed circles (●) represent the aerosol mass concentration ( $\mu\text{g}/\text{m}^3$ ).

3325

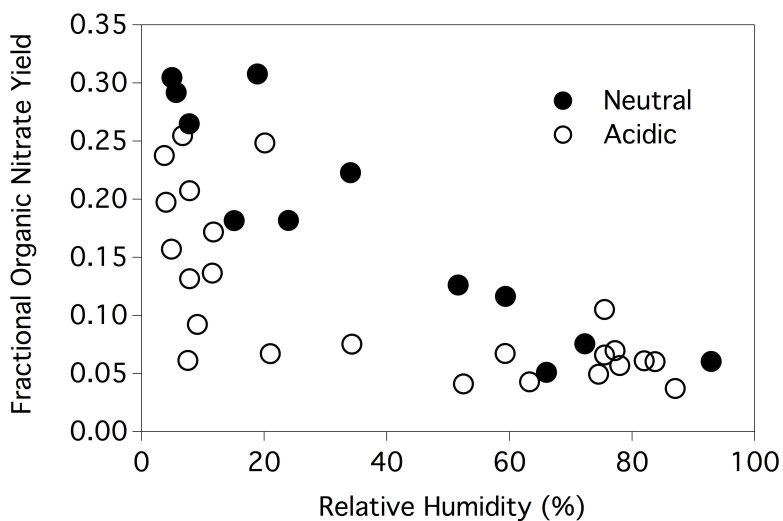


**Fig. 3.** The total organic yield as a function of chamber relative humidity for both the acidic seed aerosol (○) and neutral seed aerosol (●) experiments. Data are from multiple experiments.

3326

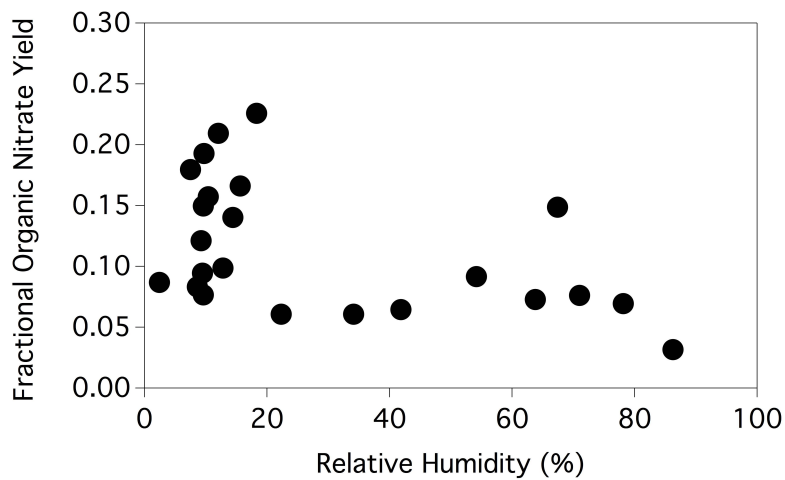


**Fig. 4.** The total organic nitrate yield as a function of chamber relative humidity for the unseeded aerosol experiments. Data are from multiple experiments.

3327

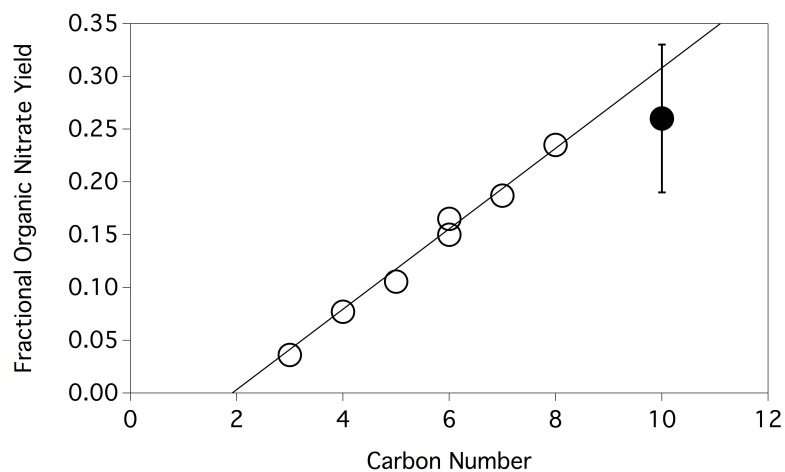


**Fig. 5.** The fractional organic nitrate yield trend from the NO addition to the peroxy radical as a function of carbon number for the original VOC species. The data and trend are described previously by Arey et al. (2001). Open circles (○) are taken from Arey et al. (2001) while the closed circle (●) is the reported value from this study ( $26 \pm 7\%$ ).

3328

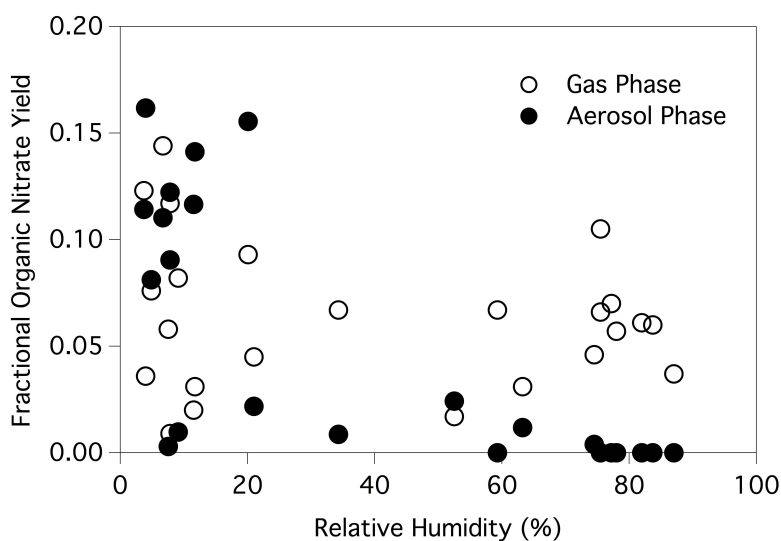


**Fig. 6.** The gas (○) and particle phase (●) organic nitrate yields as a function of experimental relative humidity for the acidic seed scenario.

3329

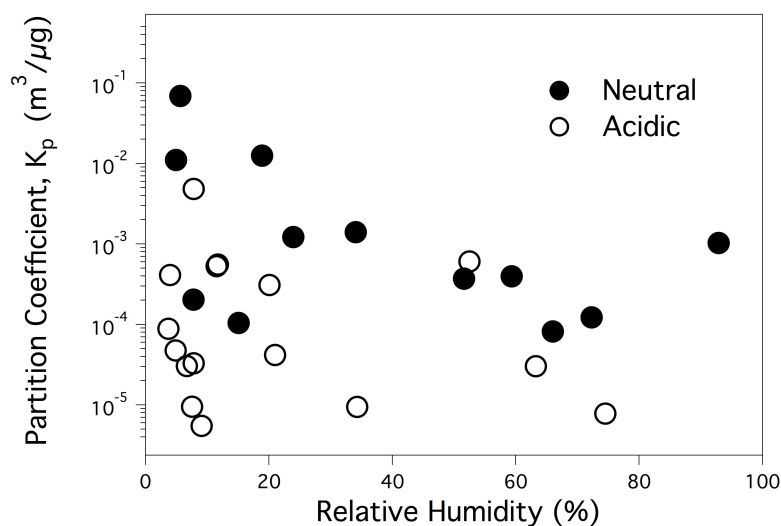
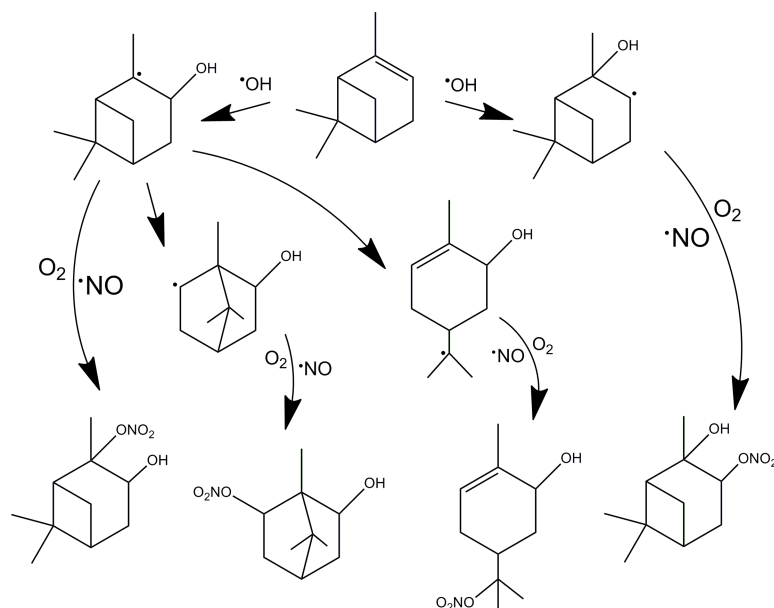


**Fig. 7.** Calculated partition coefficients ( $K_p$ ) from neutral and acidic seed aerosol experiments plotted against experiment relative humidity. Open circles (○) represent the acidic seed experiments while the closed circles (●) represent the neutral seed experiments. It is important to note that this plot does not show eight data points from the acidic seed aerosol data set which have partition coefficients of zero due to the lack of detected  $RONO_2$  in the particle phase (see Fig. 6).

3330

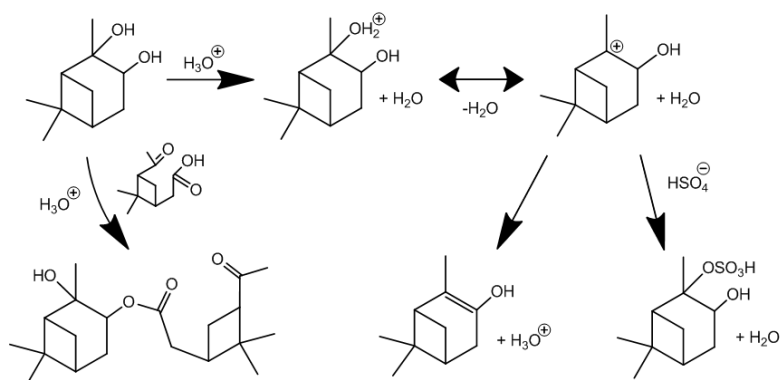






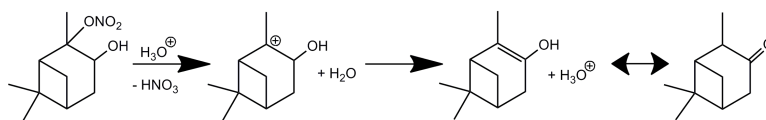
**Scheme 3.** The OH radical addition to  $\alpha$ -pinene, the possible gas phase rearrangements of the radicals formed, and the four organic nitrates isomers produced from each pathway. The proposed chemistry is based on Peeters et al. (2001).

3333



**Scheme 4.** Possible condensed phase chemistry of the expected hydrolysis product, pinane-1,2-diol. Acid-catalyzed reactions forming the pinonic acid oligomerization product from Fischer esterification (left) and elimination product (middle) are shown. The elimination product (middle) would undergo keto-enol tautomerization with the corresponding ketone compound. Nucleophilic substitution with the bisulfate ion is also shown (right). Both the organosulfate product (Surratt et al., 2008; Eddingsaas et al., 2012) and keto-enol tautomerization product (Iinuma et al., 2013) have been previously observed.

3334



**Scheme 5.** The acid-catalyzed E1 elimination mechanism for a proposed  $\alpha$ -pinene-derived organic nitrate in the condensed phase. This mechanism is in direct competition with the  $\text{S}_{\text{N}}1$  mechanism.